

Realization of the Nersesyan-Tsvelik model in (NO)[Cu(NO₃)₃]

O. Volkova,¹ I. Morozov,¹ V. Shutov,¹ E. Lapsheva,¹ P. Sindzingre,² O. Cépas,^{3,4} M. Yehia,⁵ V. Kataev,⁵ R. Klingeler,^{5,6} B. Büchner,⁵ and A. Vasiliev¹

¹Moscow State University, Moscow 119991, Russia

²Laboratoire de Physique Théorique de la Matière Condensée, UMR7600 CNRS, Université Pierre-et-Marie-Curie, Paris 6, 75252 Paris Cedex 05, France

³Institut Néel, CNRS et Université Joseph Fourier, BP 166, 38042 Grenoble, France

⁴Laboratoire J.-V. Poncelet, UMI2615 CNRS, Independent University of Moscow, Moscow 119002, Russia

⁵Leibniz Institute for Solid State and Materials Research, IFW Dresden, 01171 Dresden, Germany

⁶Kirchhoff Institute for Physics, University of Heidelberg, Im Neuenheimer Feld 227, 69120 Heidelberg, Germany

(Received 4 April 2010; published 10 August 2010)

The topology of the magnetic interactions of the copper spins in the nitrosonium nitratocuprate (NO)[Cu(NO₃)₃] suggests that it could be a realization of the Nersesyan-Tsvelik model [A. A. Nersesyan and A. M. Tsvelik, *Phys. Rev. B* **67**, 024422 (2003)], whose ground state was argued to be either a resonating valence-bond state or a valence-bond crystal. The measurement of thermodynamic and magnetic resonance properties reveals a behavior inherent to low-dimensional spin $S=\frac{1}{2}$ systems and provides indeed no evidence for the formation of long-range magnetic order down to 1.8 K.

DOI: 10.1103/PhysRevB.82.054413

PACS number(s): 75.40.Cx, 76.30.Fc

Low-dimensional quantum magnets are currently the object of intensive experimental and theoretical research. This stems from the rich physics which is displayed by these systems due to their reduced dimensionality and competing interactions which often push ordered states to very low temperatures or even preclude the formation of magnetically ordered phases at all. Geometric frustration is one of the effects which are believed to lead to possible nonclassical states. A nonclassical ground state does exist in a pure one-dimensional (1D) quantum antiferromagnet which is disordered and carries low-energy spinon excitations with fractional quantum numbers. A fundamental question is whether such nonclassical states can survive in higher dimensions and whether they realize the long-sought resonant valence bond (RVB) state.¹ The concept of RVB state is of utmost importance in modern condensed-matter physics, not only for frustrated magnetism in general but also in the context of high-temperature superconductivity of layered cupric compounds.²

An interesting model is the frustrated $S=\frac{1}{2}$ J_1 - J_2 square lattice and its extensions to further neighbor interactions. Depending on the ratio between the nearest-neighbor antiferromagnetic exchange coupling J_1 and the second-neighbor coupling J_2 , this model has a Néel ground state at weak frustration J_2/J_1 , and a stripe or collinear Néel state at strong frustration. There is a narrow region between the two phases, i.e., in the range $0.4 < J_2/J_1 < 0.6$ where there is nowadays a consensus for the absence of magnetic order. Instead, a spin liquid or a valence-bond crystal (VBC) state is discussed. However, the experimental realization of this model is still lacking. The search for experimental realizations of such a model has been pursued intensively in copper and vanadium oxides (see Ref. 3 for a recent review) but the narrow region of parameters where nonclassical states may appear is clearly a challenge for chemistry. An alternative approach to study nonclassical ground states is offered by a different J_1 - J_2 model recently introduced by Nersesyan and Tsvelik (also

named the “confederate flag” model).⁴ It differs from the J_1 - J_2 model by the spatial anisotropy of the nearest-neighbor couplings (J, J') along the horizontal and vertical directions and the same J_2 along the diagonals [see Fig. 1(a)]. The model is particularly interesting for the special ratio $J'/J_2=2$ where the ground state was first argued to be RVB in the anisotropic limit $J \gg J'=2J_2$ of weakly coupled chains.⁴ This result has been questioned since then and it was argued that the ground state could be a VBC instead^{5–10} or a gapless spin liquid.¹¹ In any case, the special condition $J'/J_2=2$ forces the effective mean field to vanish and renders the mean-field theory of coupled chains¹² which would predict long-range Neel order at zero-temperature inapplicable. Although it seems that this condition requires again a subtle fine tuning of the couplings, we shall show that it may be in fact realized

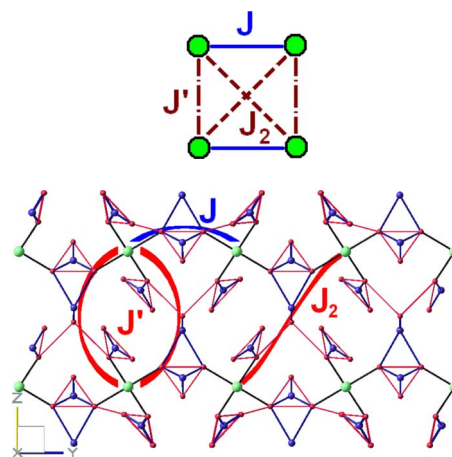


FIG. 1. (Color online) (a) Schematic representation of the anisotropic confederate flag model; (b) schematic representation of the crystal structure of (NO)[Cu(NO₃)₃]. Green spheres denote the Cu²⁺ ions. The dumbbells represent the NO⁺ cation groups. The NO₃⁻ anion groups are represented by tilted and flat triangles. Note, that $J'=2J_2$.

in a nitrosonium nitratocuprate (NO)[Cu(NO₃)₃].

Single crystals of nitrosonium nitratocuprate (NO)[Cu(NO₃)₃] were obtained by means of wet chemistry according to the procedure described in Ref. 13. The phase composition of the crystalline samples was determined by powder x-ray diffraction. The measurement was carried out on a DRON 3M diffractometer using Cu K α radiation in the 2θ range of 5°–60°. The single-phase nature of the obtained samples was confirmed by the similarity of the experimental x-ray diffraction patterns and theoretical ones calculated from single-crystal x-ray diffraction data.¹³ The bluish single crystals of (NO)[Cu(NO₃)₃] with dimensions (3–6) \times (1.5–2.5) \times (0.5–1) mm³ in the form of elongated thickened plates are not stable in air and could be safely investigated in sealed glass ampoules only. The magnetization of (NO)[Cu(NO₃)₃] has been investigated in a Quantum Design MPMS-XL5 superconducting quantum interference device magnetometer in the temperature range 1.8–300 K and electron spin resonance (ESR) data have been obtained by means of a X-band “Bruker EMX-Series” spectrometer operating at the fixed frequency $\nu=9.5$ GHz in the temperature range 3.4–300 K. In addition, the specific heat was measured at low temperatures in a Quantum Design PPMS. In all experiments, special measures have been taken against decomposition of the sample.

The crystal structure of (NO)[Cu(NO₃)₃] is represented by weakly coupled layers whose structure is shown in Fig. 1(b). Assuming, the strongest interaction J between Cu²⁺ ($S=\frac{1}{2}$) spins is provided via NO₃⁻ groups forming infinite horizontal chains along the b axis. These chains are coupled via NO₃⁻ and NO⁺ ions in the bc plane in such a manner that the vertical exchange interaction along the c axis, J' , is twice the exchange interaction along the diagonal, J_2 : there are two symmetric superexchange paths contributing to J' whereas there is only one of equivalent symmetry contributing to J_2 (assuming the main contribution comes from the paths through the NO⁺ unit). The interplane coupling along the a axis is assumed to be weak and unfrustrated. Two equivalent exchange interaction routes along this axis pass via a NO₃⁻ group whereby involving the apical oxygen at a large Cu-O distance of 2.539 Å. This is to be compared with the single exchange interaction pass via the NO₃⁻ group through the basal oxygen at a smaller Cu-O distance of 1.985 Å. Moreover, the weakness of the interplane coupling also follows from magnetic inactivity of the d_{z^2} orbital oriented along the a axis. Therefore, the topology of the (NO)[Cu(NO₃)₃] magnetic subsystem is that of the two-dimensional (2D) confederate flag model $J \gg J' = 2J_2$ [cf. Fig. 1(a)].

The temperature dependence of the specific heat C in (NO)[Cu(NO₃)₃], shown in Fig. 2, evidences an upturn at low temperatures which is moderately suppressed by an external magnetic field $\mu_0 H = 1.5$ T. This upturn can be treated as the shoulder of a Schottky anomaly as will be described below. The data taken at $\mu_0 H = 0$ T can be fitted by the sum of a linear contribution γT which is associated with the thermal excitation of one-dimensional antiferromagnetic magnons, a cubic term βT^3 related to phonons, and a Schottky contribution C_{Sch} reflecting the population of discrete energy levels. The resulting formula reads

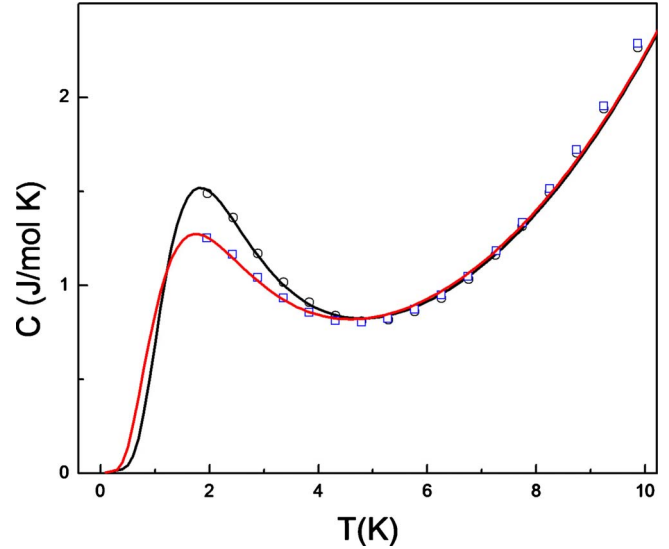


FIG. 2. (Color online) Temperature dependences of the specific heat C measured at $\mu_0 H = 0$ T (○) and $\mu_0 H = 1.5$ T (□) in (NO)[Cu(NO₃)₃], respectively. The fitting curves are shown by solid lines.

$$C = \gamma T + \beta T^3 + \alpha \frac{3}{2} R \left(\frac{\Delta}{k_B T} \right)^2 \frac{\exp\left(-\frac{\Delta}{k_B T}\right)}{\left[1 + 3 \exp\left(-\frac{\Delta}{k_B T}\right)\right]^2}$$

with α a weighting factor, R the gas constant, k_B the Boltzmann constant, and Δ the energy gap associated to the Schottky anomaly. The best fit to the experimental data is obtained with $\gamma = 0.54$ J/mol K², $\beta = 0.0016$ J/mol K⁴, $\alpha = 0.33$, and $\Delta = 5$ K. The description in terms of a Schottky anomaly is strongly corroborated by the fact that the data measured in the applied field at $\mu_0 H = 1.5$ T can be described well with the same set of parameters when the field dependence of the gap $\Delta(\mu_0 H) = \Delta(\mu_0 H = 0) - g \mu_B \mu_0 H$ is considered. In particular, the sensitivity of the Schottky anomaly to the external magnetic field indicates the magnetic origin of the relevant two-level system. Note, however, that the value of weighting factor $\alpha = 0.33$ makes it difficult to ascribe the anomaly clearly either to extrinsic or intrinsic contributions. At the same time, we mention that the shape, curvature, and field dependence of the low-temperature upturn do not suggest that the system approaches a phase transition to long-range magnetically ordered state.

The temperature dependence of the static magnetic susceptibility $\chi = M/B$ of (NO)[Cu(NO₃)₃] taken in a magnetic field of 0.1 T oriented in the bc plane is shown in Fig. 2. Upon lowering the temperature, χ first increases, passes through a broad maximum, and then rapidly increases again, showing a pronounced Curie-type behavior at low temperatures. The origin of the strong low-temperature upturn is not clear since the method of preparation excludes the presence of any other cations except Cu²⁺ and NO⁺ and any other anions except NO₃⁻ in the structure while high optical quality of the available crystals is apparent. Note, that the pronounced Curie-type behavior cannot be explained by a

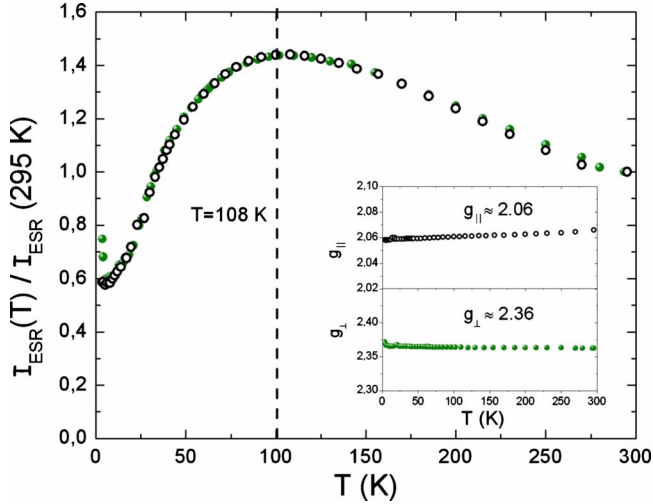


FIG. 3. (Color online) Temperature dependence of the intensity of the ESR spectra I_{ESR} normalized to the room temperature value for a magnetic field parallel (\parallel) and perpendicular (\perp) to the plane of CuO_4 plaquettes. Inset: the temperature dependence of the values of the g -factor tensor g_{\parallel} and g_{\perp} .

Schottky type anomaly with $\Delta=5$ K either. On the other hand, a broad maximum in $\chi(T)$ is a typical feature of low-dimensional magnetism and hence can be seen as a signature of reduced dimensionality of the $(\text{NO})[\text{Cu}(\text{NO}_3)_3]$ magnetic subsystem.

In order to study the *intrinsic* spin susceptibility and to obtain insights into the spin dynamics, we have performed ESR measurements of a single-crystalline sample for two orientations of the external magnetic field: The in-plane orientation parallel to the CuO_4 plaquettes, and the out-of-plane orientation, perpendicular to the CuO_4 plaquettes, \parallel and \perp , respectively. For both directions, the ESR spectrum consists of a single line (field derivative of the absorption) with the shape very close to a Lorentzian. The fit of the experimental signal to the Lorentzian derivative line profile enables an accurate determination of the intensity of the ESR signal I_{ESR} , the peak-to-peak linewidth ΔH_{pp} and the resonance field H_{res} . The g -factor tensor calculated from the resonance field as $g = h\nu / \mu_B H_{\text{res}}$ yields the values $g_{\parallel} = 2.06$ and $g_{\perp} = 2.36$. Here h is the Planck constant and μ_B is the Bohr magneton. The obtained g -factor values are typical for a Cu^{2+} ion in planar square ligand coordination.¹⁴ Remarkably, H_{res} and correspondingly the g values practically do not depend on temperature (see Fig. 3, inset), i.e., there are no indications for the development of local internal fields due to the onset of (quasi)static short- or long-range order in the entire temperature range under study. This observation strongly supports our conjecture of the low dimensionality of the spin-1/2 Heisenberg lattice in $(\text{NO})[\text{Cu}(\text{NO}_3)_3]$ where magnetic order is not expected at a finite temperature.

Generally, the integrated intensity of the ESR signal I_{ESR} is directly proportional to the static susceptibility of the spins participating in the resonance.¹⁵ Its analysis enables therefore an insight into the intrinsic magnetic susceptibility χ_{spin} of the spin lattice in $(\text{NO})[\text{Cu}(\text{NO}_3)_3]$. The temperature dependence of the I_{ESR} normalized to its value at 295 K is shown

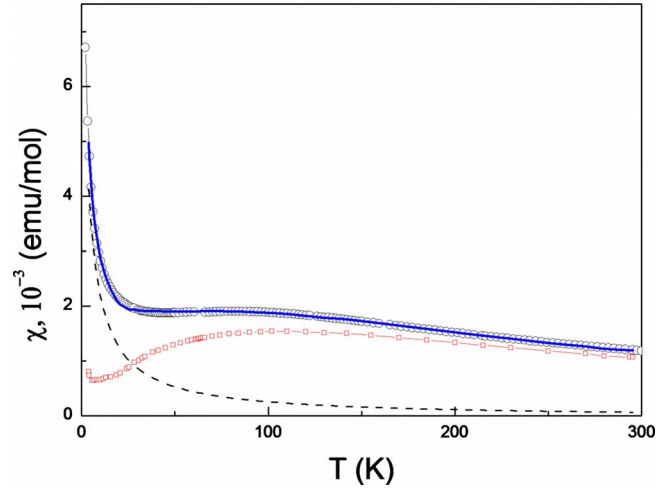


FIG. 4. (Color online) Temperature dependences of the magnetic susceptibility taken at $\mu_0 H = 0.1$ T (\circ) and of the normalized magnetic susceptibility from the ESR data (\square) of $(\text{NO})[\text{Cu}(\text{NO}_3)_3]$. The lines represent fits to the data.

in Fig. 3 for the \parallel and \perp magnetic field orientations. For both field directions, these curves are very similar and, if compared to the static magnetic measurements, show even more pronounced low dimensional behavior. Note that after subtraction of a Curie contribution the static susceptibility data resemble well the intrinsic spin susceptibility as derived from the analysis of the ESR spectra (cf. Fig. 4).

In order to extract information on the magnetic couplings, we have calculated the spin susceptibility by exact diagonalization of the Nersesyan-Tsvetlik model upon varying $\alpha = J'/J$. We have used clusters of up to 24 spins with different geometries, i.e., a square of 4×4 spins, a ladder of 8×2 spins, and a stripe of 6×4 spins with periodic boundary conditions. Because of finite-size effects, the susceptibility is exact only for $T > 2T_{\text{max}}$, where T_{max} is the temperature of the broad maximum of the susceptibility χ_{max} (see Fig. 5, right panel, solid and dashed lines for $\alpha = 0.6$, for instance). It is therefore difficult to access to the low-temperature regime where the susceptibility decreases. Nonetheless, it appears that the product $\chi_{\text{max}} T_{\text{max}}$ is less sensitive to the size and is especially useful since we know the exact Bonner-Fisher result for decoupled chains ($\alpha = 0$), given by $\chi_{\text{max}} T_{\text{max}} = 0.0941 N_A g^2 \mu_B^2 / k_B$.¹⁶ When $\alpha \neq 0$, the product is a pure function of α and is shown in Fig. 5 (left panel). One can see that $\chi_{\text{max}} T_{\text{max}}$ is approximately linear in α and the slope is found to be -0.0558 (for the 8×2), -0.0614 (for the 4×4), and -0.0607 (for the 6×4) so it is only weakly size dependent. We note that the result for $\alpha = 0$ almost coincides with Bonner Fisher for the 8×2 cluster (this is the shape with the longer chains). Combining these results, we obtain $\chi_{\text{max}} T_{\text{max}} / (N_A g^2 \mu_B^2 / k_B) = 0.0941 - 0.060\alpha$. Comparison with the experimental data, using $g^2 = 4.68$ from ESR (powder average), and conversion to standard units gives $\chi_{\text{max}} T_{\text{max}} = 0.165 - 0.105\alpha$ (emu K/mol). Given that, experimentally, $\chi_{\text{max}} T_{\text{max}} = 0.163 \pm 0.007$ emu K/mol, we can conclude that $-0.05 < \alpha < 0.09$. Our analysis therefore implies that the system is in the weak-coupling regime: given the error bar, the interchain couplings could be either ferromagnetic or antifer-

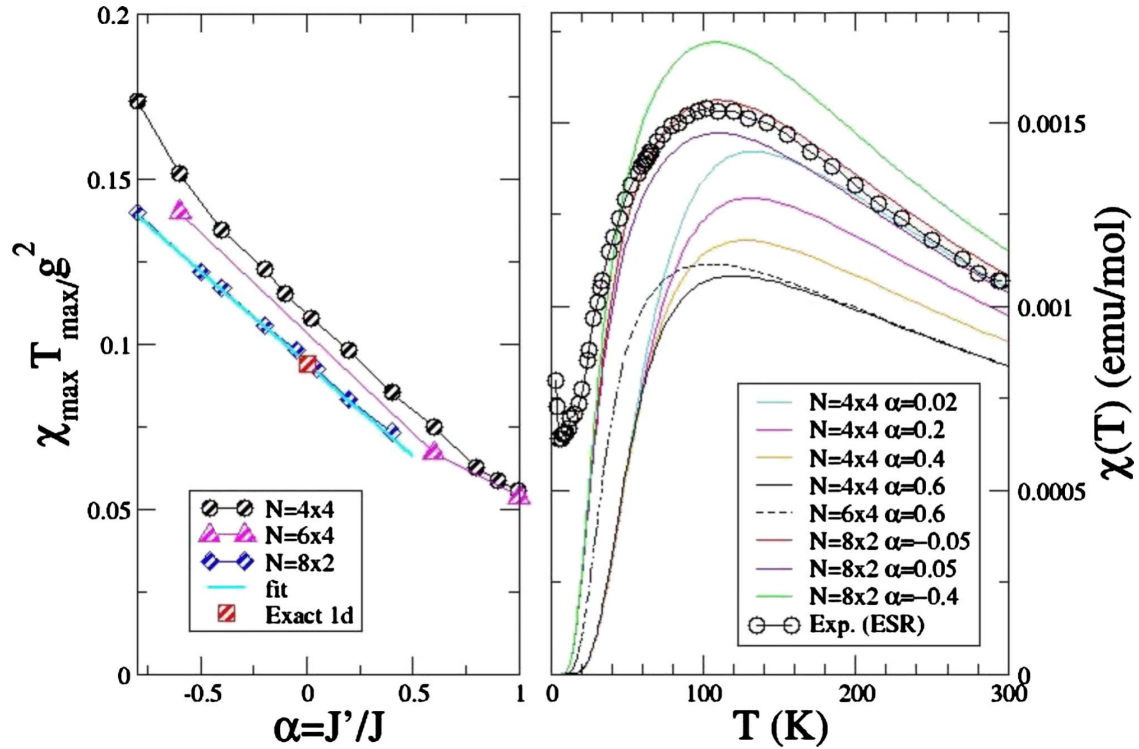


FIG. 5. (Color online) Right panel: magnetic susceptibility derived from exact diagonalizations ($\alpha = J'/J$ characterizes the interchain coupling). N is the system size and various geometries have been used [4×4 , 8×2 , 6×4]. Left panel: $\chi_{\max} T_{\max}^2 / (N_A g^2 \mu_B^2 / k_B)$ as a function of α . The exact result for decoupled chains ($\alpha=0$) is shown by a square.

romagnetic but we can exclude the strong-coupling regime. Further on, the temperature dependence of maximum susceptibility T_{\max} enables estimating the magnetic coupling J . In the case of infinite decoupled chains, $T_{\max} = 0.6408J$,¹⁷ giving $J = 170$ K in the material at hand.

Another important information can be obtained from the analysis of the linewidth ΔH_{pp} which particularly in spin-1/2 systems is mainly determined by the relaxation rate of the spin fluctuations perpendicular to the applied field. For both orientations of the external field, ΔH_{pp} shows a remarkably strong temperature dependence. In particular, below ~ 100 K the linewidth decreases by almost one order of magnitude which at first glance might be interpreted as a strong depletion of the spin-fluctuation density due to the opening of the spin gap. In fact, in this temperature regime, the $\Delta H_{pp}(T)$ dependence can be phenomenologically described reasonably well by an exponential function $\sim e^{-\Delta/T}$ with an energy gap $\Delta_{\parallel} \approx \Delta_{\perp} \sim 77$ K. However, the finite ESR intensity, i.e., the finite intrinsic spin susceptibility, observed down to the lowest temperature contradicts the spin-gap scenario. Alternatively, it is known that in a 2D antiferromagnet at temperatures far above the magnetic ordering temperature T_N the linewidth is determined mainly by the long-wave $q \approx 0$ fluctuation modes whose strength decreases with lowering the temperature as $\chi_{\text{spin}} T$ (see, e.g., Ref. 18). If a competing contribution due to the “short-wave” spin fluctuations at the staggered wave vector $q = \pi$ remain small, e.g., if the spin system is still in the regime $T \gg T_N$, one could indeed expect even for a gapless situation a progressive strong narrowing of the ESR signal due to the reduction in

both χ_{spin} and temperature. The product of the normalized ESR intensity, i.e., χ_{spin} , and temperature is shown in Fig. 6. Here, $\chi_{\text{spin}} T$ is scaled to match most closely the $\Delta H_{pp}(T)$ curves. Indeed, one observes a reasonably good qualitative agreement between $\chi_{\text{spin}} T$ and $\Delta H_{pp}(T)$ dependence. One notices that a substantial anisotropy of the linewidth at high temperatures strongly decreases at low temperatures (Fig. 5) whereas the anisotropy of the g factor stays constant (Fig. 3, inset). Such a reduction in the linewidth anisotropy is expected if the strength of $q \approx 0$ modes decreases.¹⁸

There is also a surprising similarity between the tempera-

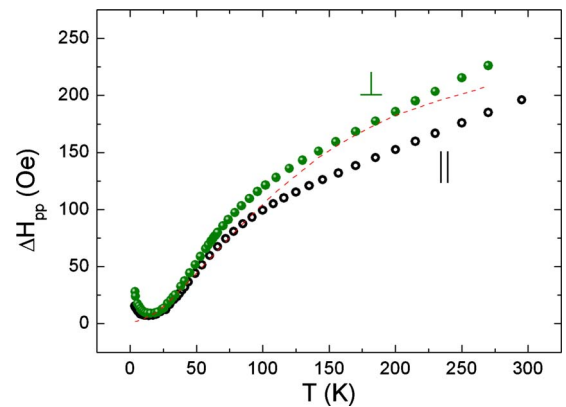


FIG. 6. (Color online) Temperature dependence of the ESR linewidth ΔH_{pp} for a magnetic field parallel and perpendicular to the plane of CuO_4 plaquettes, respectively (symbols). The dashed line shows the scaled product $\chi_{\text{spin}}(T) \cdot T$.

ture dependence of the ESR linewidth for $(\text{NO})[\text{Cu}(\text{NO}_3)_3]$ and that for some 1D spin-1/2 systems like, e.g., KCuF_3 ,^{19,20} the spin-Peierls compound CuGeO_3 ,²¹ and the quarter-filled spin ladder NaV_2O_5 .²² In all of them, a similarly strong temperature dependence of ΔH_{pp} concomitant with a strong temperature variation in the anisotropy of the linewidth is ascribed to the Dzyaloshinskii-Moriya (DM) interaction, which is allowed by the crystal symmetry in those systems. In the present case too, one can infer from the crystal structure that the DM interaction is present between spins along the chain and the D vector is staggered from bond to bond (because the Cu ion is at an inversion center) but is forbidden for the interchain couplings. Since the XZ plane passing through the middle of the Cu-Cu bond is a mirror plane, the D vector should be perpendicular to the Cu-Cu bond, anywhere inside that plane. An interesting consequence is the field-induced gap,²³ as for Cu-benzoate, although in the present case, the gap should be small with the small fields applied but it may affect the low temperature susceptibility as well.

It is of course difficult to ultimately conclude on the nature of the ground state of $(\text{NO})[\text{Cu}(\text{NO}_3)_3]$ in the view of the present experimental results. Nersesyan and Tsvetik have argued that, for small interchain couplings, the ground state remains disordered and realizes a chiral π -flux RVB spin liquid at zero temperature.⁴ However the situation is not yet settled: extension toward finite interchain couplings has led to consider other candidates for the ground state, such as VBCs (Refs. 5 and 6) or a gapless spin liquid.¹¹ If the VBC was not supported by a first density matrix renormalization group (DMRG) calculation for a spin ladder,⁸ latter works did not exclude it,¹⁰ especially if the interchain coupling is ferromagnetic,⁹ which the present work does not exclude. Although the system would be gapped in this case, the value of the gap $\Delta=5$ K estimated from the specific-heat measurements seems to be rather high. In fact, the spin gap was claimed to be extremely small from numerical studies.¹² It is also consistent with the idea that the system could be nearly critical: there are Neel states away from the special line $J'=2J_2$ but very close to it in the parameter space $J'-J_2$.^{5,6} Accordingly, the ground state of $(\text{NO})[\text{Cu}(\text{NO}_3)_3]$ could be a gapless spin liquid.¹¹ This does not contradict to results of thermodynamic and magnetic resonance measurements.

However, such a gapless spin-liquid state could be unstable to additional interactions (unfrustrated interplane interactions, DM interactions) which can result in three-dimensional long-range magnetic order at lower temperatures.

In conclusion, we have found that a nitrosonium nitratocuprate $(\text{NO})[\text{Cu}(\text{NO}_3)_3]$ seems to be a good realization of the Nersesyan-Tsvetik model in the weak-coupling regime: main magnetic couplings of the Heisenberg model were found to be $J=170$ K and $-0.05 < \alpha=J'/J < 0.09$. Obviously, our work which introduces this very interesting material calls for further experimental and theoretical studies of its magnetic properties. It is clear that a precise determination of the interchain couplings deserves further investigations such as calculations of the electronic-structure and neutron-scattering experiments. In addition, departures from the Heisenberg model in the form of Dzyaloshinskii-Moriya interactions may exist in the system (as indicated by ESR) and thus can also contribute to the low-temperature susceptibility. This issue needs to be clarified by, e.g., high-field magnetic studies and symmetry analysis of the spin structure. In any case, owing to the special geometry of the Nersesyan-Tsvetik model, the interchain interactions are not only weak but also strongly frustrated, thus making an RVB or VBC states possible. Experimentally, indeed, no indications of the phase transition were found down to 1.8 K despite strong antiferromagnetic couplings, and it is an interesting issue as to whether such states are realized or not in the present material.

Note added in proof. Recently, we received a note from A. Tsirlin and colleagues that questions the model presented here. They admitted that, claiming $J'/J_2=2$ we neglect an interaction between NO_3 units flared-out of the plane of Fig. 1(b) in different directions. This may contribute to J' but may not contribute to J_2 . Thus, this remains an open question as to whether the model proposed provides a coherent interpretation of the full susceptibility.

We acknowledge the support of the present work by DFG through Grants No. 486 RUS 113/982/0-1 and No. KL 1824/2, RFBR through Grant No. 09-02-91336, and Federal Target Program of Russian Federation through Grant No. 02.740.11.0219.

¹P. W. Anderson, *Science* **235**, 1196 (1987).

²J. G. Bednorz and K. A. Müller, *Z. Phys.* **64**, 189 (1986).

³A. A. Tsirlin and H. Rosner, *Phys. Rev. B* **79**, 214417 (2009).

⁴A. A. Nersesyan and A. M. Tsvetik, *Phys. Rev. B* **67**, 024422 (2003).

⁵P. Sindzingre, *Phys. Rev. B* **69**, 094418 (2004).

⁶O. A. Starykh and L. Balents, *Phys. Rev. Lett.* **93**, 127202 (2004).

⁷S. Moukouri and J. V. Alvarez, [arXiv:cond-mat/0403372](https://arxiv.org/abs/cond-mat/0403372) (unpublished).

⁸H.-H. Hung, C.-D. Gong, Y.-C. Chen, and M.-F. Yang, *Phys. Rev. B* **73**, 224433 (2006).

⁹T. Hikihara and O. A. Starykh, *Phys. Rev. B* **81**, 064432 (2010).

¹⁰E. H. Kim, O. Legeza, and J. Solyom, *Phys. Rev. B* **77**, 205121 (2008); G.-H. Liu, H.-L. Wang, and G.-S. Tian, *ibid.* **77**, 214418 (2008).

¹¹S. Moukouri, *Phys. Rev. B* **70**, 014403 (2004).

¹²H. J. Schulz, *Phys. Rev. Lett.* **77**, 2790 (1996).

¹³K. O. Znamenkov, I. V. Morozov, and S. I. Troyanov, *Russ. J. Inorg. Chem.* **49**, 172 (2004).

¹⁴J. R. Pilbrow, *Transition Ion Electron Paramagnetic Resonance* (Clarendon Press, Oxford, 1990).

¹⁵A. Abragam and B. Bleaney, *Electron Paramagnetic Resonance of Transition Ions* (Oxford University Press, London, 1970).

- ¹⁶J. C. Bonner and M. E. Fisher, *Phys. Rev.* **135**, A640 (1964).
- ¹⁷D. C. Johnston, R. K. Kremer, M. Troyer, X. Wang, A. Klümper, S. L. Bud'ko, A. F. Panchula, and P. C. Canfield, *Phys. Rev. B* **61**, 9558 (2000).
- ¹⁸P. M. Richards and M. B. Salamon, *Phys. Rev. B* **9**, 32 (1974).
- ¹⁹I. Yamada, H. Fujii, and M. Hidaka, *J. Phys.: Condens. Matter* **1**, 3397 (1989).
- ²⁰M. V. Eremin, D. V. Zakharov, H.-A. Krug von Nidda, R. M. Eremina, A. Shuvaev, A. Pimenov, P. Ghigna, J. Deisenhofer, and A. Loidl, *Phys. Rev. Lett.* **101**, 147601 (2008).
- ²¹I. Yamada, M. Nishi, and J. Akimitsu, *J. Phys.: Condens. Matter* **8**, 2625 (1996).
- ²²M. Lohmann, H.-A. Krug von Nidda, M. V. Eremin, A. Loidl, G. Obermeier, and S. Horn, *Phys. Rev. Lett.* **85**, 1742 (2000).
- ²³M. Oshikawa and I. Affleck, *Phys. Rev. Lett.* **79**, 2883 (1997).